

Article

The Properties of Poly(ester amide)s Based on Dimethyl 2,5-Furandicarboxylate as a Function of Methylene Sequence Length in Polymer Backbone

Konrad Walkowiak ^{1,*} , Izabela Irska ¹ , Agata Zubkiewicz ², Jerzy Dryzek ³ and Sandra Paszkiewicz ¹ 

¹ Department of Materials Technologies, Faculty of Mechanical Engineering and Mechatronics, West Pomeranian University of Technology, PL 70310 Szczecin, Poland; izabela.irska@zut.edu.pl (I.I.); sandra.paszkiewicz@zut.edu.pl (S.P.)

² Department of Physics, Faculty of Mechanical Engineering and Mechatronics, West Pomeranian University of Technology, PL 70311 Szczecin, Poland; azubkiewicz@zut.edu.pl

³ Institute of Nuclear Physics Polish Academy of Sciences, PL 31342 Krakow, Poland; jerzy.dryzek@ifj.edu.pl

* Correspondence: wk42388@zut.edu.pl; Tel.: +48-91-449-45-89

Abstract: A series of poly(ester amide)s based on dimethyl furan 2,5-dicarboxylate (DMFDC), 1,3-propanediol (PDO), 1,6-hexylene glycol (HDO), and 1,3-diaminopropane (DAP) were synthesized via two-step melt polycondensation. The phase transition temperatures and structure of the polymers were studied by differential scanning calorimetry (DSC). The positron annihilation lifetime spectroscopy (PALS) measurement was carried out to investigate the free volume. In addition, the mechanical properties of two series of poly(ester amide)s were analyzed. The increase in the number of methylene groups in the polymer backbone resulted in a decrease in the values of the transition temperatures. Depending on the number of methylene groups and the content of the poly(propylene furanamide) (PPAF), both semi-crystalline and amorphous copolymers were obtained. The free volume value increased with a greater number of methylene groups in the polymer backbone. Moreover, with a lower number of methylene groups, the value of the Young modulus and stress at break increased.

Keywords: poly(ester amide)s; a number of methylene groups; biopolymers; 2,5-furandicarboxylic acid; thermal properties; mechanical performance; PALS



Citation: Walkowiak, K.; Irska, I.; Zubkiewicz, A.; Dryzek, J.; Paszkiewicz, S. The Properties of Poly(ester amide)s Based on Dimethyl 2,5-Furandicarboxylate as a Function of Methylene Sequence Length in Polymer Backbone. *Polymers* **2022**, *14*, 2295. <https://doi.org/10.3390/polym14112295>

Academic Editor: Alberto Frache

Received: 26 April 2022

Accepted: 3 June 2022

Published: 5 June 2022

Publisher's Note: MDPI stays neutral with regard to jurisdictional claims in published maps and institutional affiliations.



Copyright: © 2022 by the authors. Licensee MDPI, Basel, Switzerland. This article is an open access article distributed under the terms and conditions of the Creative Commons Attribution (CC BY) license (<https://creativecommons.org/licenses/by/4.0/>).

1. Introduction

Most polymers are based on petrochemicals, but the increasing environmental awareness and dwindling fossil fuel resources have made it clear that this needs to be changed. Consequently, there is a growing interest in the use of renewable raw materials for fuels, chemicals, and polymer materials [1]. In 2004, the US Department of Energy recognized 2,5-furandicarboxylic acid (FDCA) as one of the twelve most important renewable materials [2]. The FDCA and its derivatives find application in the synthesis of bio-based polyurethanes, polyamides, and especially polyesters. The similar structure of FDCA to terephthalic acid (TPA) popularized the synthesis of materials such as poly(ethylene 2,5-furanoate) (PEF) and poly(propylene furanoate) (PPF), which are more environmentally friendly equivalents of poly(ethylene terephthalate) (PET) and poly(propylene terephthalate) (PPT) [1,3,4]. Moreover, due to the heteroatom in the structure of the furan ring, polyesters based on FDCA exhibit excellent gas barrier properties [5,6]. For example, PEF has 11 times better barrier properties to O₂, and 19 times better to CO₂ than PET [7–9]. As a result, it can be used in the production of films, bottles, and fibers [10].

In order to increase the applicability of furan-based polymers, attention has been paid to poly(ester amide)s (PEA)s. This polymeric class has excellent mechanical and thermal properties, thanks to intermolecular hydrogen bonds that increase interactions between

the polymer chains [1]. However, obtaining polyamides and PEA from FDCA has proved to be quite a challenge [11]. It is due to the side reactions, including decarboxylation occurring around 200 °C and the N-methylation of FDCA, that occur [12], whereby the synthesized PEAs have a low molecular weight and are amorphous or have a low degree of crystallinity [13]. Therefore, in the last few years, several attempts to synthesize polyamides and PEAs based on FDCA and its derivatives have been described (e.g., solution polymerization [14], enzymatic polymerization [12,15,16], direct polycondensation [17], and solid-state polymerization [13,18]). One of the strategies involves enzymatic polymerization, which uses an immobilized form of *Candida Antarctica* lipase b, which serves as a catalyst for polycondensation between dimethyl furan 2,5-dicarboxylate DMFDC and aliphatic diamines [15,19]. This reaction takes place under mild conditions, which solves the problem of decarboxylation and the N-methylation of FDCA. However, materials obtained with the use of this strategy were amorphous or characterized by slow crystallization unless treated with solvents. Kluge et al. [20] synthesized semicrystalline PEAs using symmetric amido diol, 1,10-decanediol, and DMFDC via melt polycondensation. The addition of amide groups caused an increase in the degree of crystallinity and improved the thermal and mechanical properties of the material. The crystallization of PEA can occur with a sufficiently high molecular weight and tight packing of molecules, and the formation of hydrogen bonds between the amide protons and the oxygen atom in the furan ring may appear. Moreover, semicrystalline PEA based on FDCA can only be obtained if there is enough space between the amide group and the furan ring [21]. Increasing the number of methylene groups in the aliphatic diols may provide enough space and makes it easier for PEA to crystallize. However, the parity of the number of methyl groups has a significant effect on the crystallization and phase transition temperatures [22]. Polyesters with an even number of methylene groups have a higher value of phase transition temperatures and crystallize more easily than polyesters with an odd number of methylene groups [22], and this effect should also be observed for PEAs.

Therefore, we have compared two series of PEAs, i.e., with an odd number of the methylene group poly(trimethylene 2,5-furandicarboxylate)-co-poly(propylene furanamide) (PTF-co-PPAF) and with an even number of the methylene group poly(hexamethylene 2,5-furandicarboxylate)-co-poly(propylene furanamide) (PHF-co-PPAF). The influence of various aliphatic diols on the selected properties of materials was investigated, in particular the thermal behavior, free volume changes, and mechanical performance. The details about the molecular structure and physico-chemical properties for these particular series of PEAs were already published in [11,21].

2. Materials and Methods

2.1. Synthesis of Copoly(amide-esters)

The series of poly(trimethylene 2,5-furanoate)-co-poly(propylene furanamide) (PTF-co-PPAF) and of poly(hexylene 2,5-furanoate)-co-poly(propylene furanamide) (PHF-co-PPAF) copolymers were obtained from dimethyl furan 2,5-dicarboxylate (DMFDC, 99%, Henan Coreychem Co., Ltd., Zhengzhou, China), 1,3-propylene glycol (bio-PDO, DuPont Tate & Lyle BioProducts, Loudon, OH, USA), 1,6-hexylene glycol (HDO, Rennovia Inc., Santa Clara, CA, USA), and 1,3-diaminopropane (DAP, >99%, Sigma Aldrich, Steinheim am Albuch, Baden-Württemberg, Germany). Materials were synthesized via two-step melt polycondensation in a 1 dm³ high-pressure reactor (Autoclave Engineers, Erie, PA, USA). In the first step, transesterification between DMFDC, bio-PDO, and DAP in the presence of titanium (IV) butoxide (Ti(OBu)₄, Fluka[®] Analytical) as a catalyst and Irganox 1010 (Ciba-Geigy, Switzerland) as an antioxidant was carried out for PTF-co-PPAF. In turn, to obtain PHF-co-PPAF, bio-PDO was replaced with HDO. Transesterification was performed at the range of temperature of 160–190 °C, and the end of the first stage was signaled by distillation of 90% of the theoretical value of the by-product. The second portion of the catalyst (Ti(OBu)₄) was added before the second step. During polycondensation, the temperature was gradually increased to 220 °C for PTF-co-PPAF and 240 °C for PHF-

co-PPAF, and pressure was reduced below 20 Pa for both series. The second stage was finished when the proper value of the melt viscosity was acquired, which was evaluated by observation of a stirring torque change. The materials were then pressed from the reactor into the water bath. The extruded materials were granulated in a laboratory mill and injected into a dumbbell-shaped sample, type A3, using a Boy 15 (Dr BOY GmbH & Co., Neustadt, Germany) for a tensile test. The injection parameters are summarized in Table 1. The chemical structure of the copolymers is presented in Figure 1.

Table 1. Injection molding parameters of copolymers.

Series	T _i [°C]	P _i [MPa]	T _f [°C]	P _d [Mpa]	t _i [s]	t _c [s]
PTF-co-PPAF	195	85	30	30	6	15
PHF-co-PPAF	180	40	30	25	5	30

T_i—temperature of injection; P_i—injection pressure; T_f—temperature of form; P_d—holding down pressure; t_i—time of injection; t_c—time of cooling.

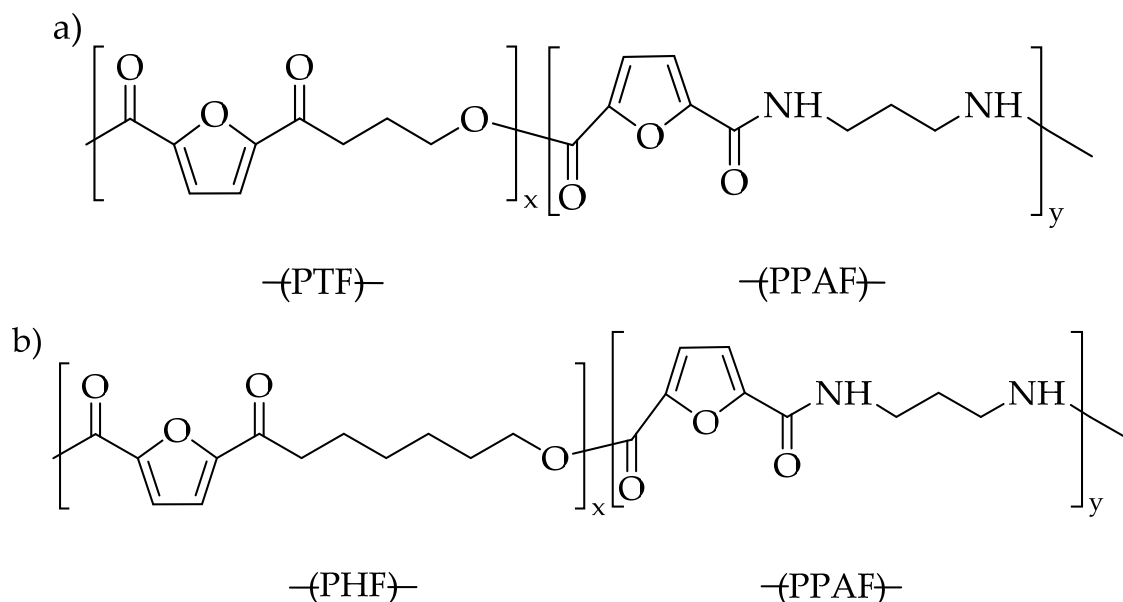


Figure 1. Chemical structure of: PTF-co-PPAF (a); PHF-co-PPAF (b).

2.2. Characterization Methods

The chemical structure of the obtained materials was studied by ¹H NMR. Before the experiment, samples were subjected to extraction for 24 h. ¹H NMR spectroscopy was performed on a Bruker spectrometer (Karlsruhe, Germany) at 400 MHz using chloroform-d CDCl₃ at a concentration of 10 mg/mL with a few drops of trifluoroacetic acid (CF₃COOH) to dissolve the samples. Tetramethylsilane (TMS) was used as a reference for the internal chemical shift. The mole fractions of the PPAF segments were calculated from the determined integral intensities of the characteristic peaks, according to Equation (1):

$$W_{\text{PTF-co-PPAF}} = \frac{2I_x}{2I_x + I_y} \times 100\% \text{ or } W_{\text{PHF-co-PPAF}} = \frac{I_x}{I_x + 2I_y} \times 100\% \quad (1)$$

where I_x and I_y are integral signal intensities that correspond to peaks of 3.63 ppm and 2.26 ppm for PTF and PTF-co-PPAF, respectively, and 2.15 ppm and 4.32 for PHF and its based copolymers, respectively.

Differential scanning calorimetry (DSC) was performed using DSC 204 F1 Phoenix (Netzsch, Selb, Germany). A total of 10 mg of each sample were encapsulated in aluminum pans and analyzed in a temperature range from −75 °C to 250 °C with a speed of

10 °C/min. The measurement was carried out under nitrogen flow in a heat/cool/heat cycle. The degree of crystallinity was calculated from Equation (2):

$$x_c = \frac{\Delta H_m - \Delta H_x}{\Delta H_m^0} \quad (2)$$

where ΔH_m and ΔH_x are the melt and cold crystallization or crystallization enthalpy, respectively, and ΔH_m^0 is the heat of fusion of the 100% crystalline polyester: for PTF it is 142 J/g [23] and for PHF it is 143 J/g [24].

The thermo-oxidation was investigated by employing TGA 92-16.18 Setaram (Caluire-et-Cuire, France). The measurements were carried out in an oxidizing atmosphere, i.e., dry, synthetic air ($N_2:O_2 = 80:20$ vol.%) at a flow rate of 20 mL/min, with a heating rate of 10 °C/min in the temperature range of 20–700 °C. Measurements were conducted under the PN-EN ISO 11358:2004 standard.

Positron annihilation lifetime spectroscopy (PALS) measurements were carried out on a TechnoAp digital positron lifetime spectrometer with a timing resolution of 190 ps. The $^{22}NaCl$ between two thin Kapton foils with a thickness of 7 μm was the source of the positron. For the detection of the annihilation and 1.27 MeV gamma photons, two Hamamatsu H3378-50 photomultipliers coupled with a single crystal of BaF2 scintillators from KristalKort were used. Spectras obtained from the measurement were deconvoluted using the LT-Polymer code [25].

The static mechanical properties were investigated using Autograph AG-X plus (Shimadzu, Kyoto, Japan), which is equipped with an optical extensometer, 1 kN Shimadzu load cell, and Trapezium X software. In the beginning, the materials were extended to 1% with a crosshead speed of 1 mm/min. Then, the stress–strain curves for the materials were obtained at a rate of 5 mm/min. The reported values are an average of the five test specimens. The measurements were performed according to PN-EN ISO 527.

3. Results

3.1. Structure and Composition

The chemical structure and composition of the PTF, PHF, and copoly(ester amide)s were confirmed by 1H NMR. The 1H NMR spectra of the polyesters and copolymers with the lowest and highest content of PPAF are shown in Figure 2. Furthermore, the composition of the obtained materials can be found in Table 2. The signal at 7.24 ppm for PTF and 7.19 for PHF is assigned to the protons of the furan ring. PTF and PHF differed in the signals derived from the methylene group. The peaks occurring at 4.52 ppm and 2.27 ppm are associated with the propylene glycol subunit for PTF, while the peaks at 4.33, 1.79, and 1.48 ppm correspond to the protons of the methylene groups in the hexylene glycol subunit for PHF. However, a weak signal at 2.1 ppm was observed in PHF, which is associated with the central methylene group belonging to 1,3-propanediol. The PTF- or PHF-based copolymers showed signals associated with PPAF, the peak from the protons of the methylene groups adjacent to the nitrogen atom appeared at 3.63 ppm, and the signal from the amide proton was visible at 3.98 ppm. The calculated molar fractions of PPAF were slightly lower than the theoretical values, which could have resulted from the formation of by-products and the lower molecular weight of these materials. For sure, the obtained poly(ester amide)s were found to be random copolymers. This was caused by the almost equal reactivities of the monomers and the random transesterification reaction during the polycondensation process.

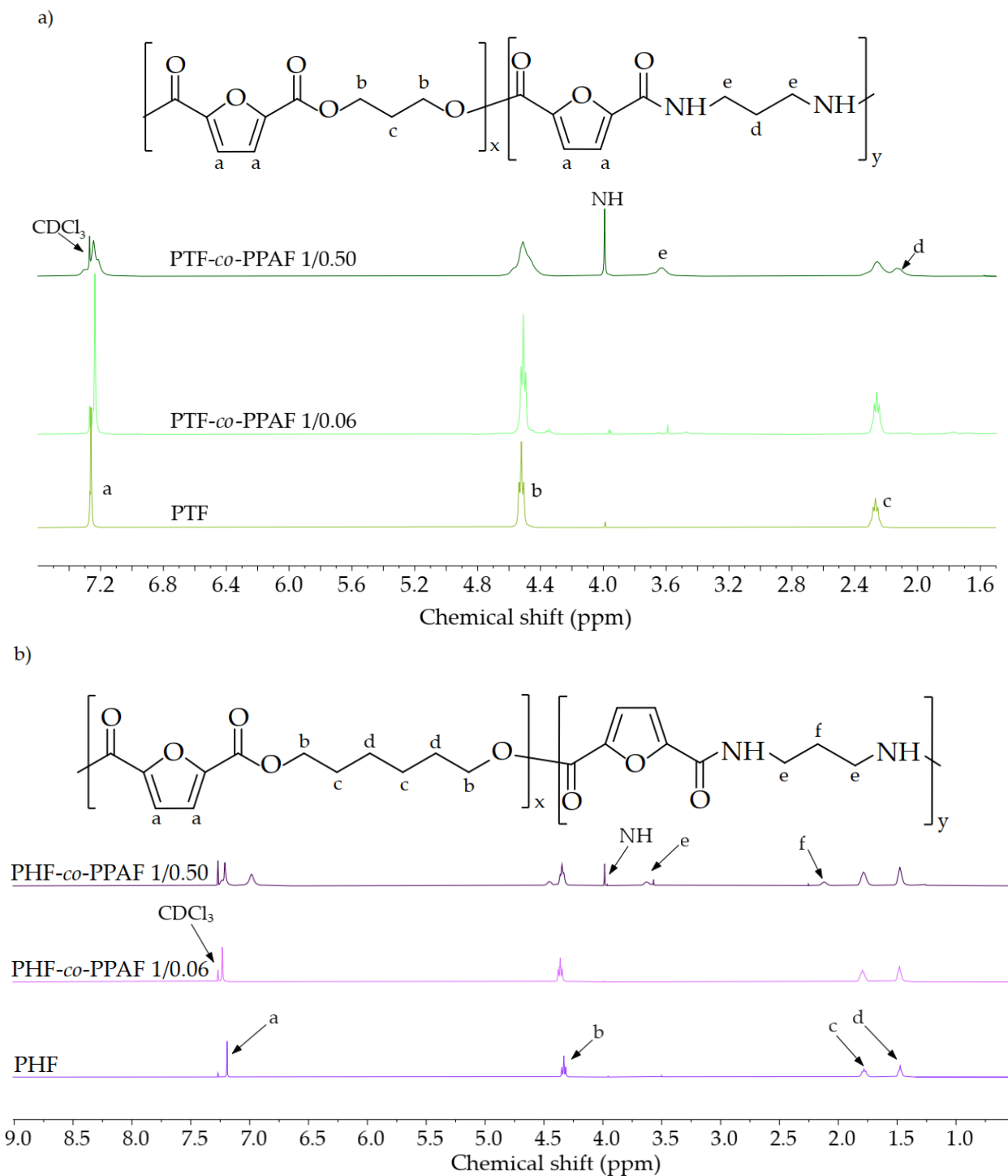


Figure 2. ¹H-NMR spectra of PTF, PTF-co-PPAF 1/0.06, PTF-co-PPAF 1/0.50 (a), and PHF, PHF-co-PPAF 1/0.06, PHF-co-PPAF 1/0.50 (b).

Table 2. Composition of PTF, PHF, and copoly(ester amide)s based on them.

Material	W _{polyester} (mol.%)	W _{PPAF} (mol.%)	W _{PPAF} ^{NMR} (mol.%)
PTF	100	0	0
PTF-co-PPAF 1/0.06	94	6	4.76
PTF-co-PPAF 1/0.16	84	16	16.67
PTF-co-PPAF 1/0.25	75	25	25.37
PTF-co-PPAF 1/0.50	50	50	45.03
PHF	100	0	0
PHF-co-PPAF 1/0.06	94	6	7.47
PHF-co-PPAF 1/0.16	84	16	15.25
PHF-co-PPAF 1/0.25	75	25	24.24
PHF-co-PPAF 1/0.50	50	50	45.05

W_{polyester}—mole fractions of PTF or PHF units; W_{PPAF}—mole fractions of PPAF units; W_{PPAF}^{NMR}—mole fraction of PPAF units determined by ¹H-NMR.

3.2. Thermal Properties

In order to investigate the phase transition temperatures and the structure of the synthesized polymers and copolymers, the DSC measurement was performed. The DSC thermograms recorded during the second heating and cooling are shown in Figure 3. Results from the DSC analysis are summarized in Table 3. It is clearly visible that the PHF and PHF-based copolymers exhibited a lower value of glass transition compared to the PTF and PTF-based PEAs since an increase in the alkyl chain length changed the flexibility of the chain due to the internal plasticization of the polymer backbone [3]. Moreover, one can observe that the addition of the PPAF content to the neat polyesters caused an increase in the value of the glass transition temperature in both series. It was due to the hydrogen bonds of the amide groups which increased the stiffness of the molecular chains [3]. Therefore, PTF-co-PPAF 0.50 had the highest glass transition temperature (73.9 °C) compared to the rest of the synthesized polymers. The PTF and PTF-co-PPAF copolymers did not crystallize due to the insufficient space between the amide group and the furan ring and also because polyesters with an odd number of methylene groups do not crystallize as well as polyesters with an even number of methylene groups [22]. Moreover, polyesters with a longer methylene unit sequence length had a better regularity of molecular chains that made it easier for the polyesters to crystallize. Only PHF, PHF-co-PPAF 1/0.06, and PHF-co-PPAF 1/0.16 showed a crystalline structure, although the degree of crystallinity decreased with increasing PPAF content. It was caused by thermodynamic interaction between PHF and PPAF, in which the amorphous PPAF units reduced the thickness of the crystals and became less stable [21,26]. That is why the degree of crystallinity between PHF and PHF-co-PPAF 1/0.16 differed significantly, about 24.7%. Contrary to PHF, which crystallized during cooling, PHF-co-PPAF 1/0.06 and PHF-co-PPAF 1/0.16 were characterized by cold crystallization due to a limited crystallization ability. The cold crystallization temperature increased with a higher molar fraction of PPAF, but the enthalpy of the cold crystallization decreased. Moreover, the melting temperature also decreased with an increasing PPAF content. In addition, the characteristic temperatures of the 5% and the 50% mass loss designated from TGA are shown in Table 3. PTF and its copolymers exhibited higher thermal stability in comparison to PHF and the series of PHF-co-PPAF. This was due to the lower number of methylene groups of PTF and the copolyesters based on it, providing more rigidity to the polymer chains. A more detailed investigation for each series can be found in [11,21].

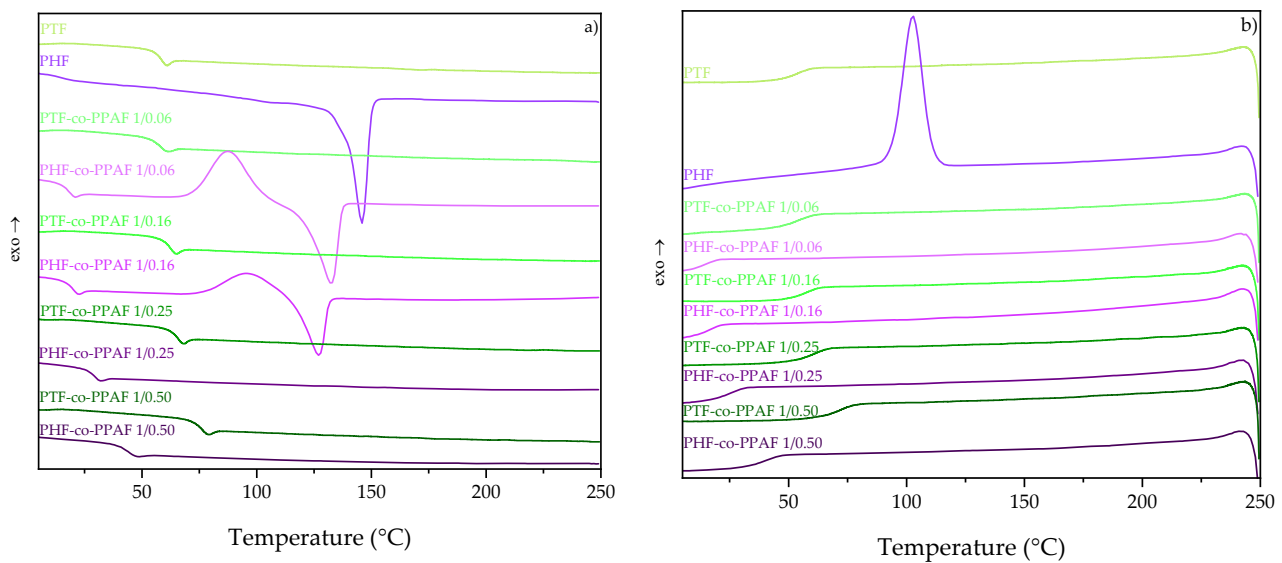


Figure 3. DSC thermograms recorded during second heating (a), and cooling (b).

Table 3. Thermal properties determined from 2nd heating and cooling thermograms for synthesized polyesters and copolymers.

Sample	T _g (°C)	ΔC _p (J/g °C)	T _{cc} (°C)	ΔH _{cc} (J/g)	T _c (°C)	ΔH _c (J/g)	T _m (°C)	ΔH _m (J/g)	χ _c (%)	T _{5%} (°C)	T _{50%} (°C)
PTF	56.6	0.40	-	-	-	-	-	-	-	364 ^A	392 ^A
PTF-co-PPAF 1/0.06	55.9	0.39	-	-	-	-	-	-	-	366 ^A	397 ^A
PTF-co-PPAF 1/0.16	60.1	0.47	-	-	-	-	-	-	-	367 ^A	400 ^A
PTF-co-PPAF 1/0.25	63.7	0.41	-	-	-	-	-	-	-	367 ^A	408 ^A
PTF-co-PPAF 1/0.50	73.9	0.41	-	-	-	-	-	-	-	360 ^A	401 ^A
PHF	15.0	0.12	-	-	103.0	41.9	146.0	36.3	25.4	354 ^B	388 ^B
PHF-co-PPAF 1/0.06	17.0	0.41	87.0	32.5	-	-	133.0	34.8	1.6	349 ^B	386 ^B
PHF-co-PPAF 1/0.16	19.0	0.33	96.0	18.1	-	-	127.0	19.0	0.7	352 ^B	388 ^B
PHF-co-PPAF 1/0.25	28.0	0.32	-	-	-	-	-	-	-	350 ^B	388 ^B
PHF-co-PPAF 1/0.50	43.0	0.30	-	-	-	-	-	-	-	334 ^B	383 ^B

T_g—glass transition temperature; ΔC_p—change of heat capacity; T_{cc}, ΔH_{cc}—cold crystallization temperature and the corresponding enthalpy of crystallization; T_c, ΔH_c—crystallization temperature and the corresponding enthalpy of crystallization; T_m, ΔH_m—melting temperature and the corresponding enthalpy of melting, T_{5%}—temperature of 5% mass loss, and T_{50%}—temperature of 50% mass loss designated at the oxidizing atmosphere for ^A the series of PTF-co-PPAF [11] and ^B for the series of PHF-co-PPAF [21].

3.3. Positron Annihilation Lifetime Spectroscopy

Positron lifetime spectra were carried out to determine the change of the free volume in the synthesized polymers. They were measured at room temperature and described considering three lifetime components. The first and second components were shorter lifetimes: τ₁ (the annihilation of the para-positronium, p-Ps) and τ₂ (the annihilation of the free position). The third lifetime component τ₃ was attributed to the ortho-positronium (o-Ps) and was commonly related to the annihilation in free volume. The values of τ₃ and I₃ are important because they are used to describe the pick-off process. In this process, the positron in Ps annihilates with an electron other than its associated partner and with the opposite spin during Ps collisions with the surrounding molecules [27]. The pick-off process is represented by a model which uses τ₃ to calculate the free volume radius (R) (Equation (3)):

$$\tau_3[ns] = 0.5 \left[1 - \frac{R}{R + \Delta} + \frac{1}{2\pi} \sin\left(2\pi \frac{R}{R + \Delta}\right) \right] \quad (3)$$

where $\Delta = 0.1656$ nm is the parameter determined experimentally for the other molecular solids [27], and I_3 is used for the calculation of free volume fractions (f_v) (Equation (4)):

$$f_v = aV_v I_3 \quad (4)$$

where the size of the free volume cavities $V_v = 4\pi R^3/3$ is expressed in \AA^3 and the coefficient $a = 0.0018$ [28].

The lifetime and intensity values of the components, the free volume radius (R), and the free volume fractions (f_v) are summarized in Table 4. The PALS measurement for PHF-co-PPAF was described in our previous article [21]. The τ_3 and the intensity of the component corresponding to the o-PS annihilation (I_3) were in the range of 1.50 to 1.56 ns and 12.6 to 15.6% for PTF and the series of PTF-co-PPAF, respectively. The values of τ_3 did not differ significantly, but the values of I_3 decreased with increasing PPAF concentrations due to the lower density of the free-volume holes. Similar to τ_3 , the R value for PTF-co-PPAF had a similar value, which indicated no influence of the PPAF content on the free volume radius, Table 4. However, with a higher molar fraction of PPAF in a series of PTF-co-PPAF, the value of the free volume fraction decreased. Before comparing the series of PTF-PPAF and PHF-co-PPAF, it should be noted that PHF, PHF-co-PPAF 1/0.06, and PHF-co-PPAF 1/0.16 have a glass transition temperature below room temperature, at which the measurement was performed. For this reason, these polymers, despite being semicrystalline, did not have a lower value of the free volume radius and free volume fraction in comparison to PHF-co-PPAF 1/0.25 and PHF-co-PPAF 1/0.50. The polymer with the highest value of τ_3 and I_3 was PHF which differed from PTF by about 0.18 ns and 4.8%, respectively. Moreover, PHF and the series of PHF-co-PPAF had more methylene groups than PTF and PTF-co-PPAF, which affected the value of R and f_v . The free volume radius value was slightly higher for the series of PHF-co-PPAF, but the value of the free volume fraction was significantly higher in comparison to the series of PTF-co-PPAF. This was due to the reduction of the ester group density with the increase in methylene groups, which reduced the stiffness of the molecular chains and increased the value of f_v .

Table 4. Results obtained from positron annihilation lifetime spectroscopy.

Sample	τ_1 (ps)	I_1 (%)	τ_2 (ps)	I_2 (%)	τ_3 (ns)	I_3 (%)	R (\AA)	V_v (\AA^3)	f_v (%)
PTF	206.5 ± 6.7	34.7 ± 2.0	418.6 ± 10.3	49.7 ± 1.8	1.54 ± 0.01	15.6 ± 0.61	0.24 ± 0.01	0.06 ± 0.01	1.59 ± 0.02
PTF-co-PPAF 1/0.06	207.8 ± 7.3	35.1 ± 1.9	424.5 ± 9.4	50.5 ± 1.8	1.56 ± 0.02	14.5 ± 0.56	0.24 ± 0.01	0.06 ± 0.01	1.51 ± 0.04
PTF-co-PPAF 1/0.16	200.4 ± 5.4	31.5 ± 1.4	406.3 ± 6.2	54.0 ± 1.3	1.51 ± 0.01	14.5 ± 0.41	0.24 ± 0.01	0.05 ± 0.01	1.4 ± 0.04
PTF-co-PPAF 1/0.25	192.4 ± 8.0	31.4 ± 1.9	407.4 ± 9.0	54.9 ± 1.8	1.53 ± 0.02	13.6 ± 0.54	0.24 ± 0.01	0.06 ± 0.01	1.37 ± 0.03
PTF-co-PPAF 1/0.50	188.7 ± 7.6	30.8 ± 1.8	403.7 ± 8.1	56.6 ± 1.7	1.50 ± 0.01	12.6 ± 0.46	0.24 ± 0.01	0.05 ± 0.01	1.21 ± 0.03
PHF	192.3 ± 11.9	27.0 ± 2.7	395.1 ± 11.6	52.6 ± 2.5	1.72 ± 0.01	20.4 ± 1.02	0.26 ± 0.01	0.07 ± 0.01	2.64 ± 0.03
PHF-co-PPAF 1/0.06	184.0 ± 6.0	26.3 ± 1.4	381.5 ± 5.3	54.3 ± 1.2	1.67 ± 0.01	19.4 ± 0.49	0.25 ± 0.01	0.07 ± 0.01	2.34 ± 0.03
PHF-co-PPAF 1/0.16	193.0 ± 9.2	29.1 ± 1.9	389.2 ± 7.1	50.8 ± 1.8	1.68 ± 0.01	20.1 ± 0.71	0.25 ± 0.01	0.07 ± 0.01	2.49 ± 0.03
PHF-co-PPAF 1/0.25	191.3 ± 9.2	31.3 ± 2.3	399.5 ± 11.4	49.9 ± 2.1	1.67 ± 0.01	18.8 ± 0.84	0.25 ± 0.01	0.07 ± 0.01	2.27 ± 0.03
PHF-co-PPAF 1/0.50	186.5 ± 4.9	27.9 ± 1.1	393.4 ± 4.2	53.0 ± 1.0	1.65 ± 0.01	19.1 ± 0.38	0.25 ± 0.01	0.07 ± 0.01	2.28 ± 0.03

$\tau_1, I_1, \tau_2, I_2, \tau_3, I_3$, positron lifetime and intensity of components, corresponding to the shortest lifetime component (p-Ps), the intermediate component, and the pick-off annihilation of the o-Ps component, respectively; R , free volume radius; V_v , size of the free volume cavities; f_v , free volume fractions.

3.4. Mechanical Properties

The representative stress–strain curves of the synthesized polymers are shown in Figure 4. The values of the tensile modulus (E), tensile strength at yield (σ_y), elongation at yield (ϵ_y), tensile strength at break (σ_b), and elongation at break (ϵ_b) are summarized in Table 5. Unlike PTF and its copolymers, PHF and the series of PHF-co-PPAF exhibited a yield point. The value of E and σ_b were higher for the PTF-co-PPAF copolymers due to the higher stiffness caused by a lesser number of methylene groups in comparison to the other synthesized polymers. Moreover, as the PPAF content increased for both series of the copolymers, their E value also increased significantly compared to the neat polyesters. The reason for this was the strong intermolecular hydrogen bonding of the amide groups in the microstructure [29]. However, with an increasing fraction of PPAF, the tensile strength of

the copolymers decreased compared to the PTF and PHF; a similar effect was observed by Yang et al. [30]. The PHF and PHF-co-PPAF copolymers had a higher value of elongation at break than PTF and the copolymers based on it. This was due to the higher mobility of their molecular chains caused by a greater number of methylene groups. In addition, only PHF showed a strain-hardening effect caused by the orientation of the macromolecular chains and crystallization during stretching. The samples were conditioned at room temperature, which was higher than the glass transition temperature of PHF, PHF-co-PPAF 1/0.06, and PHF-co-PPAF 1/0.16, before the mechanical property testing. This may have increased the degree of crystallinity resulting from the cold crystallization of these samples. Therefore, an increase in the value of Young’s modulus was observed for PHF-co-PPAF 1/0.06 and PHF-co-PPAF 1/0.16 compared to PHF, while the Young’s modulus value decreased after the PPAF content exceeded 0.16 mol.%. Above this content, the obtained copolymers were fully amorphous, as explained in the DSC section.

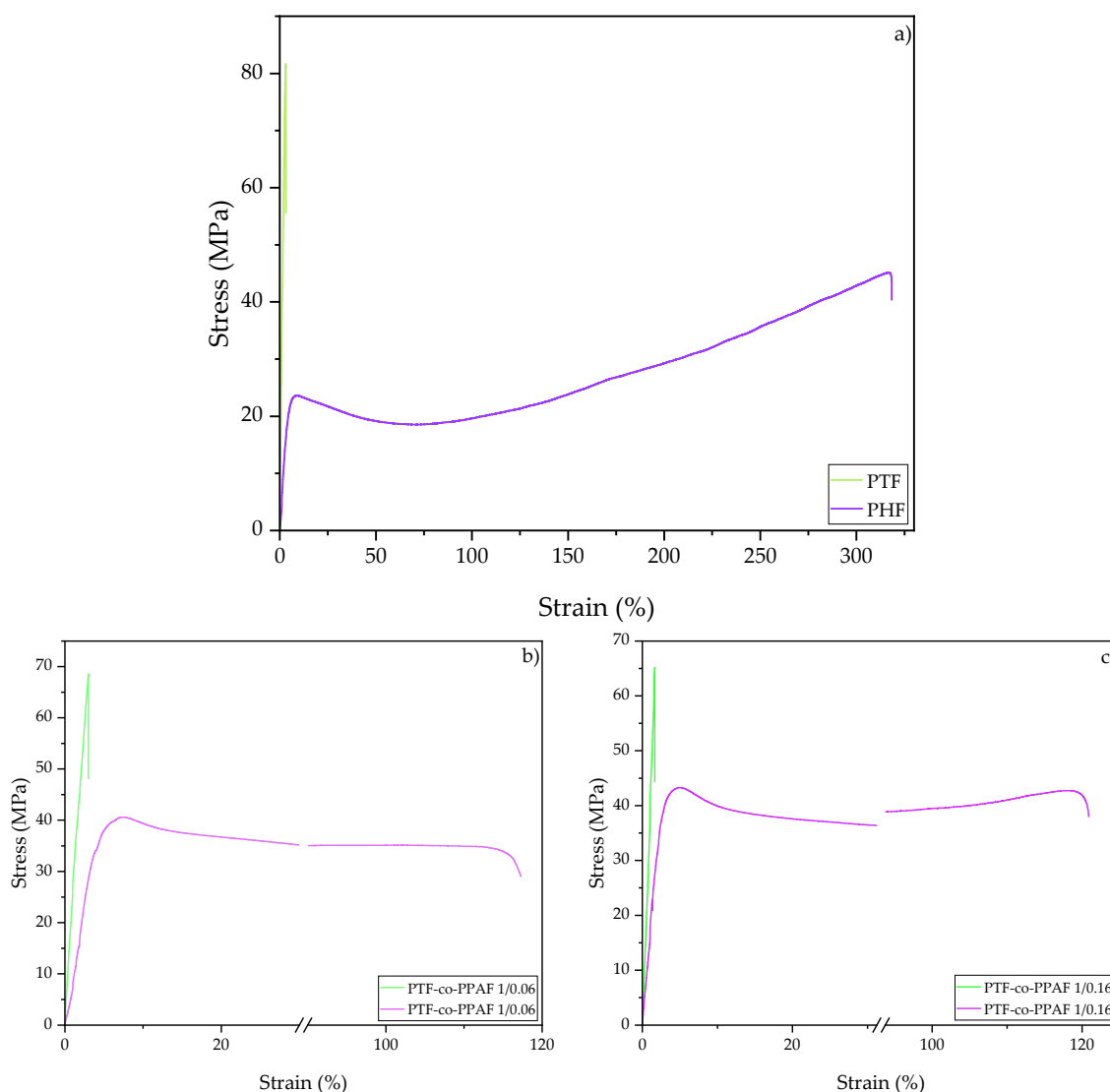


Figure 4. Cont.

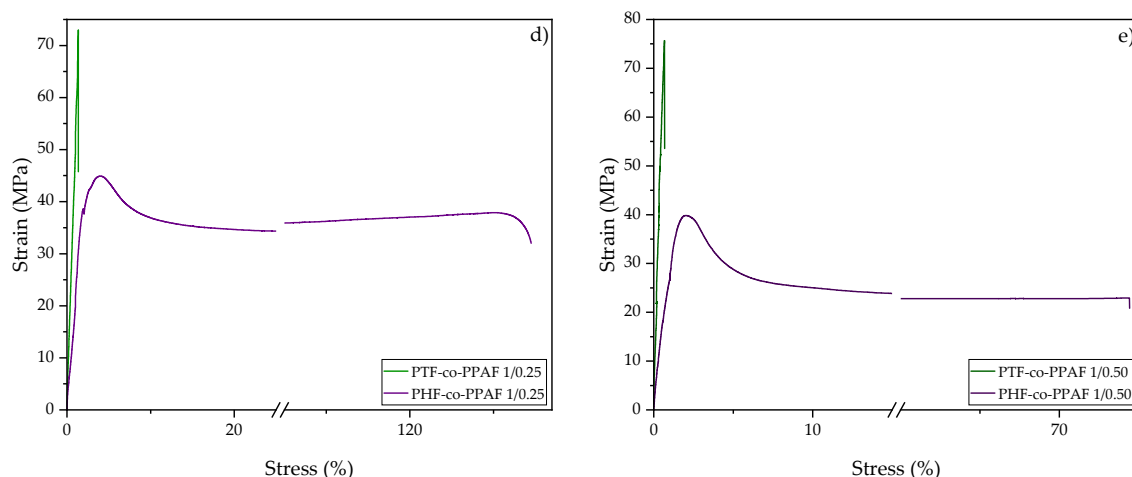


Figure 4. Representative tensile stress–strain curves for: (a) PTF, PHF; (b) PTF-co-PPAF 1/0.06, PHF-co-PPAF 1/0.06; (c) PTF-co-PPAF 1/0.16, PHF-co-PPAF 1/0.16; (d) PTF-co-PPAF 1/0.25, PHF-co-PPAF 1/0.25; (e) PTF-co-PPAF 1/0.50, PHF-co-PPAF 1/0.50.

Table 5. Mechanical properties of PTF, PHF, and copolymers based on them.

Sample	E (GPa)	σ_y (MPa)	ϵ_y (%)	σ_b (MPa)	ϵ_b (%)
PTF	2.5 ± 0.4	-	-	81.6 ± 1.6	3.1 ± 0.2
PTF-co-PPAF 1/0.06	2.2 ± 0.2	-	-	68.5 ± 1.0	3.0 ± 0.1
PTF-co-PPAF 1/0.16	2.6 ± 0.2	-	-	64.7 ± 0.6	1.6 ± 0.1
PTF-co-PPAF 1/0.25	3.0 ± 0.2	-	-	72.8 ± 0.7	1.4 ± 0.1
PTF-co-PPAF 1/0.50	3.6 ± 0.1	-	-	75.6 ± 0.9	0.7 ± 0.1
PHF	0.4 ± 0.1	23.6 ± 0.9	8.8 ± 1.0	45.3 ± 2.7	319.2 ± 13.3
PHF-co-PPAF 1/0.06	0.8 ± 0.1	42.4 ± 1.8	6.1 ± 0.9	39.1 ± 4.1	146.3 ± 14.9
PHF-co-PPAF 1/0.16	1.7 ± 0.2	43.3 ± 2.6	5.0 ± 0.4	38.8 ± 3.6	106.6 ± 13.7
PHF-co-PPAF 1/0.25	1.3 ± 0.2	43.7 ± 1.0	2.1 ± 0.2	39.4 ± 2.8	147.1 ± 24.6
PHF-co-PPAF 1/0.50	1.0 ± 0.2	38.4 ± 2.2	2.5 ± 0.7	25.8 ± 3.1	75.3 ± 10.3

E, Young's modulus; σ_y , stress at yield; ϵ_y , elongation at yield; σ_b , stress at break; ϵ_b , elongation at break.

4. Conclusions

Two series of copoly(ester amide)s synthesized by two-step polycondensation were compared in terms of thermal behavior, free volume changes, and mechanical performance. The morphology and phase transition temperatures were investigated by DSC. PHF and the materials based on PHF containing a lower amount of PPAF, i.e., 0.06 mol.% and 0.16 mol.%, can crystallize. This is a result of the better regularity of the molecular chains and the appropriate distance between the amide group and the furan ring. However, the addition of a higher content of PPAF disturbed the crystallization process and caused an increase in the glass transition temperature. The materials with a greater number of methylene groups had a higher value of the free volume fraction and the volume radius, measured by PALS, in comparison to the materials with a lesser number of methylene groups. The f_v decreased with increasing PPAF content. Moreover, the relationship between the mechanical properties and the number of methylene groups was proven. The synthesized materials with a higher number of methylene groups also had a higher elongation at the break value than the polymers with a lower number of methylene groups.

Author Contributions: Writing—original draft preparation, K.W.; writing—review and editing, investigation, and formal analysis, I.I.; investigation, J.D.; writing—review and editing and investigation, A.Z.; writing—review and editing, supervision, and funding acquisition, S.P. All authors have read and agreed to the published version of the manuscript.

Funding: This study was financed by the National Science Centre within project SONATA no. 2018/31/D/ST8/00792.

Institutional Review Board Statement: Not applicable.

Informed Consent Statement: Not applicable.

Data Availability Statement: The data presented in this study are available on request from the corresponding author. After publication, the data will be kept in the open repositories by means of Mendeley Data and RepOD.

Conflicts of Interest: The authors declare no conflict of interest.

References

1. Papadopoulos, L.; Klonos, P.A.; Kluge, M.; Zamboulis, A.; Terzopoulou, Z.; Kourtidou, D.; Magaziotis, A.; Chrissafis, K.; Kyritsis, A.; Bikiaris, D.N.; et al. Unlocking the Potential of Furan-Based Poly(Ester Amide)s: An Investigation of Crystallization, Molecular Dynamics and Degradation Kinetics of Novel Poly(Ester Amide)s Based on Renewable Poly(Propylene Furanoate). *Polym. Chem.* **2021**, *12*, 5518–5534. [[CrossRef](#)]
2. Werpy, T.; Petersen, G. *Top Value Added Chemicals from Biomass: Volume I*; US National Renewable Energy Lab: Golden, CO, USA, 2004; pp. 1–76. [[CrossRef](#)]
3. Papamokos, G.; Dimitriadis, T.; Bikiaris, D.N.; Papageorgiou, G.Z.; Floudas, G. Chain Conformation, Molecular Dynamics, and Thermal Properties of Poly(n-Methylene 2,5-Furanoates) as a Function of Methylene Unit Sequence Length. *Macromolecules* **2019**, *52*, 6533–6546. [[CrossRef](#)]
4. Loos, K.; Zhang, R.; Pereira, I.; Agostinho, B.; Hu, H.; Maniar, D.; Sbirrazzuoli, N.; Silvestre, A.J.D.; Guigo, N.; Sousa, A.F. A Perspective on PEF Synthesis, Properties, and End-Life. *Front. Chem.* **2020**, *8*, 585. [[CrossRef](#)] [[PubMed](#)]
5. Guidotti, G.; Soccio, M.; García-Gutiérrez, M.C.; Ezquerro, T.; Siracusa, V.; Gutiérrez-Fernández, E.; Munari, A.; Lotti, N. Fully Biobased Superpolymers of 2,5-Furandicarboxylic Acid with Different Functional Properties: From Rigid to Flexible, High Performant Packaging Materials. *ACS Sustain. Chem. Eng.* **2020**, *8*, 9558–9568. [[CrossRef](#)] [[PubMed](#)]
6. Burgess, S.K.; Leisen, J.E.; Kraftschik, B.E.; Mubarak, C.R.; Kriegel, R.M.; Koros, W.J. Chain Mobility, Thermal, and Mechanical Properties of Poly(Ethylene Furanoate) Compared to Poly(Ethylene Terephthalate). *Macromolecules* **2014**, *47*, 1383–1391. [[CrossRef](#)]
7. Papageorgiou, G.Z.; Papageorgiou, D.G.; Terzopoulou, Z.; Bikiaris, D.N. Production of Bio-Based 2,5-Furan Dicarboxylate Polyesters: Recent Progress and Critical Aspects in Their Synthesis and Thermal Properties. *Eur. Polym. J.* **2016**, *83*, 202–229. [[CrossRef](#)]
8. Paszkiewicz, S.; Irska, I.; Piesowicz, E. Environmentally Friendly Polymer Blends Based on Post-Consumer Glycol-Modified Poly(Ethylene Terephthalate) (PET-G) Foils and Poly(Ethylene 2,5-Furanoate) (PEF): Preparation and Characterization. *Materials* **2020**, *13*, 2673. [[CrossRef](#)]
9. Burgess, S.K.; Karvan, O.; Johnson, J.R.; Kriegel, R.M.; Koros, W.J. Oxygen Sorption and Transport in Amorphous Poly(Ethylene Furanoate). *Polymer* **2014**, *55*, 4748–4756. [[CrossRef](#)]
10. Walkowiak, K.; Irska, I.; Zubkiewicz, A.; Rozwadowski, Z.; Paszkiewicz, S. Influence of Rigid Segment Type on Copoly(Ether-Ester) Properties. *Materials* **2021**, *14*, 4614. [[CrossRef](#)]
11. Zubkiewicz, A.; Irska, I.; Miadlicki, P.; Walkowiak, K.; Rozwadowski, Z.; Paszkiewicz, S. Structure, Thermal and Mechanical Properties of Copoly(Ester Amide)s Based on 2,5-furandicarboxylic Acid. *J. Mater. Sci.* **2021**, *56*, 19296–19309. [[CrossRef](#)]
12. Jiang, Y.; Maniar, D.; Woortman, A.J.J.; Loos, K. Enzymatic Synthesis of 2,5-Furandicarboxylic Acid-Based Semi-Aromatic Polyamides: Enzymatic Polymerization Kinetics, Effect of Diamine Chain Length and Thermal Properties. *RSC Adv.* **2016**, *6*, 67941–67953. [[CrossRef](#)]
13. Cao, M.; Zhang, C.; He, B.; Huang, M.; Jiang, S. Synthesis of 2,5-Furandicarboxylic Acid-Based Heat-Resistant Polyamides under Existing Industrialization Process. *Macromol. Res.* **2017**, *25*, 722–729. [[CrossRef](#)]
14. Luo, K.; Wang, Y.; Yu, J.; Zhu, J.; Hu, Z. Semi-Bio-Based Aromatic Polyamides from 2,5-Furandicarboxylic Acid: Toward High-Performance Polymers from Renewable Resources. *RSC Adv.* **2016**, *6*, 87013–87020. [[CrossRef](#)]
15. Jiang, Y.; Maniar, D.; Woortman, A.J.J.; Alberda Van Ekenstein, G.O.R.; Loos, K. Enzymatic Polymerization of Furan-2,5-Dicarboxylic Acid-Based Furanic-Aliphatic Polyamides as Sustainable Alternatives to Polyphthalamides. *Biomacromolecules* **2015**, *16*, 3674–3685. [[CrossRef](#)]
16. Maniar, D.; Silvianti, F.; Ospina, V.M.; Woortman, A.J.J.; van Dijken, J.; Loos, K. On the Way to Greener Furanic-Aliphatic Poly(Ester Amide)s: Enzymatic Polymerization in Ionic Liquid. *Polymer* **2020**, *205*, 122662. [[CrossRef](#)]
17. Mitiakoudis, A.; Gandini, A. Characterization of Furanic. *Macromolecules* **1991**, *24*, 830–835. [[CrossRef](#)]
18. Endah, Y.K.; Han, S.H.; Kim, J.H.; Kim, N.K.; Kim, W.N.; Lee, H.S.; Lee, H. Solid-State Polymerization and Characterization of a Copolyamide Based on Adipic Acid, 1,4-Butanediamine, and 2,5-Furandicarboxylic Acid. *J. Appl. Polym. Sci.* **2016**, *133*, 4–11. [[CrossRef](#)]
19. Huang, W.; Hu, X.; Zhai, J.; Zhu, N.; Guo, K. Biorenewable Furan-Containing Polyamides. *Mater. Today Sustain.* **2020**, *10*, 100049. [[CrossRef](#)]
20. Kluge, M.; Papadopoulos, L.; Magaziotis, A.; Tzetzis, D.; Zamboulis, A.; Bikiaris, D.N.; Robert, T. A Facile Method to Synthesize Semicrystalline Poly(Ester Amide)s from 2,5-Furandicarboxylic Acid, 1,10-Decanediol, and Crystallizable Amido Diols. *ACS Sustain. Chem. Eng.* **2020**, *8*, 10812–10821. [[CrossRef](#)]

21. Zubkiewicz, A.; Irska, I.; Walkowiak, K.; Dryzek, J.; Paszkiewicz, S. Bio-Renewable Furan-Based Poly(Ester Amide)s: Synthesis, Structure, Spectroscopic and Mechanical Properties of Poly(Hexylene 2,5-Furandicarboxylate)-Co-Poly(Propylene Furanamide)s (PHF-Co-PPAF). *Express Polym. Lett.* **2022**, in press.
22. Zhang, Q.; Song, M.; Xu, Y.; Wang, W.; Wang, Z.; Zhang, L. Bio-Based Polyesters: Recent Progress and Future Prospects. *Prog. Polym. Sci.* **2021**, *120*, 101430. [[CrossRef](#)]
23. Papageorgiou, G.Z.; Papageorgiou, D.G.; Tsanaktsis, V.; Bikiaris, D.N. Synthesis of the Bio-Based Polyester Poly(Propylene 2,5-Furan Dicarboxylate). Comparison of Thermal Behavior and Solid State Structure with Its Terephthalate and Naphthalate Homologues. *Polymer* **2015**, *62*, 28–38. [[CrossRef](#)]
24. Papageorgiou, G.Z.; Tsanaktsis, V.; Papageorgiou, D.G.; Chrissafis, K.; Exarhopoulos, S.; Bikiaris, D.N. Furan-Based Polyesters from Renewable Resources: Crystallization and Thermal Degradation Behavior of Poly(Hexamethylene 2,5-Furan-Dicarboxylate). *Eur. Polym. J.* **2015**, *67*, 383–396. [[CrossRef](#)]
25. Knasy, J. LT Programs. Available online: <https://prac.us.edu.pl/~kksy/index.php?id=ltpolym> (accessed on 16 November 2010).
26. Hoffman, J.D.; Weeks, J.J. Melting Process and the Equilibrium Melting Temperature of Polychlorotrifluoroethylene. *J. Res. Natl. Bur. Stand. Sect. A Phys. Chem.* **1962**, *66*, 13–28. [[CrossRef](#)]
27. Irska, I.; Paszkiewicz, S.; Pawlikowska, D.; Dryzek, J.; Linares, A.; Nogales, A.; Ezquerra, T.A.; Piesowicz, E. Relaxation Behaviour and Free Volume of Bio-Based Poly(Trimethylene Terephthalate)-Block-Poly(Caprolactone) Copolymers as Revealed by Broadband Dielectric and Positron Annihilation Lifetime Spectroscopies. *Polymer* **2021**, *229*, 123949. [[CrossRef](#)]
28. Wang, Y.Y.; Nakanishi, H.; Jean, Y.C.; Sandreczki, T.C.; Douglas, M. Positron Annihilation in Amine-Cured Epoxy Polymers-Pressure Dependence. *J. Polym. Sci. Part B Polym. Phys.* **1990**, *28*, 1431–1441. [[CrossRef](#)]
29. Gao, H.; Bai, Y.; Liu, H.; He, J. Mechanical and Gas Barrier Properties of Structurally Enhanced Poly(Ethylene Terephthalate) by Introducing 1,6-Hexylenediamine Unit. *Ind. Eng. Chem. Res.* **2019**, *58*, 21872–21880. [[CrossRef](#)]
30. Yang, Z.Y.; Chou, Y.L.; Yang, H.C.; Chen, C.W.; Rwei, S.P. Synthesis and Characterization of Thermoplastic Poly(Ester Amide)s Elastomer (Tpeae) Obtained from Recycled Pet. *J. Renew. Mater.* **2021**, *9*, 867–880. [[CrossRef](#)]